The Packing of Triacylglycerols from SAXS Measurements: Application to the Structure of 1,3-Distearoyl-2-oleoyl-*sn*-glycerol Crystal Phases

Oleksandr O. Mykhaylyk*,† and Ian W. Hamley

Department of Chemistry, University of Leeds, Leeds, LS2 9JT, U.K.

Received: December 22, 2003; In Final Form: March 16, 2004

An approach by which electron density profiles of triacylglycerols (TAGs) can be reconstructed from X-ray diffraction data has been applied to analyze lamellar structures formed by 1,3-distearoyl-2-oleoyl-*sn*-glycerol (StOSt). The method is analogous to one previously used to analyze lipid bilayer structures. Based on the structure of tristearin molecules crystallized in the β phase, the projection of the electron density profile along the layer normal in structures with a lamellar packing of the TAG has been calculated for both tilted and nontilted arrangements of the molecules. This enables the position of glycerol groups to be identified in the electron density profile reconstructed from the first few 00*l* lamellar peaks measured by small-angle X-ray scattering (SAXS). It is demonstrated that structure amplitudes of both two-chain- and three-chain-length layers formed by the same equally tilted TAG molecules follow a unique curve on a plot of the structure amplitudes versus the scattering wave vector. The approach is applied to examine the complex polymorphism of StOSt during crystallization. Time-resolved SAXS/WAXS measurements have been performed during isothermal crystallization (from the liquid phase at 55 °C) at different temperatures (0−22.5 °C), followed by annealing at 30 °C. It is concluded that six phases (α_2, α_1, γ, β', β_1, and β_2) and one metastable structure can be formed by StOSt molecules through polymorphic transformations. Fourier reconstructed projections of the electron density profile along the layer normal show that symmetry-related pairs of StOSt molecules adopt a two-chain packing motif in the α_1 phase and a three-chain packing motif in the more stable γ, β', and β phases of StOSt. In accordance with the electron density profile, the unstable α_2 phase appearing at the initial stage of the crystallization can be ascribed to three-chain packing, which is probably the result of the twisted acyl chains of StOSt molecules. A combination of structural parameters obtained in the study, together with models for terrace-like arrangements of terminal methyl groups developed by de Jong et al., allowed the structure of γ and β phases to be clarified. The driving forces for the polymorphic transformations taking place during crystallization and a schematic diagram of phase transitions are discussed.

Introduction

Due to their widespread occurrence in natural fats, triacylglycerols (TAGs) occupy a dominant position among other glycerolipids used in human nutrition, pharmaceuticals, and cosmetics. Usually, natural fats containing triacylglycerols demonstrate a complex polymorphism,[1] and knowledge of the phase transition mechanisms is necessary to control crystallization behavior of TAGs, which is an important factor that determines physical and chemical properties of food and cosmetic products. Among different methods, such as infrared (IR) spectroscopy, nuclear magnetic resonance (NMR), differential scanning calorimetry (DSC), and X-ray diffraction (XRD), used to analyze polymorphic transformations of triacylglycerols,[2] the XRD methods are the most informative about crystal structure. Due to X-ray single-crystal studies, first reported by Vand and Bell[3] and followed by several other studies,[4−6] the structure of saturated triacylglycerols in the most stable crystal form is available.

Despite significant progress made recently in both crystal growth and X-ray single-crystal investigations of triacylglycerols, only the structure of stable forms of TAGs (β and β') can be obtained from these studies.[7−10] However, to understand polymorphic transformations of TAGs, the crystal structure of various unstable phases has to be obtained where the growth of single crystals convenient for X-ray single-crystal measurements is unlikely. Thus, most structural information about these phases available from XRD is limited to results of X-ray powder diffraction measurements. Two positionally separated sets of diffraction maxima can be identified in XRD powder patterns of TAGs: at small angles of X-ray scattering corresponding to the longitudinal order of triacylglycerols packed in layers and at large angles of X-ray scattering related to the transverse order of the molecules within the layers. To understand the packing motif of TAGs, a great deal of attention has been paid to the position of the lamellar peaks observed in small-angle X-ray scattering (SAXS) profiles to derive geometrical relations between the periodicity of layers, the composition of the acyl chain, and the conformational order of triacylglycerols.[2] Although the method to determine the projection of the electron density profile along a particular crystallographic direction from diffraction peak intensities is well-known,[11] the intensities of the TAG lamellar peaks that contain information about the projection of the electron density profile along the layer normal have not been analyzed. However, this approach is actively used in the related subject of lipid packing in biological membranes,[12,13] where single crystals cannot be grown a priori. The

* Corresponding author. Tel.: +44 113 3431151. Fax: +44 113 3436565. E-mail: O.Mykhaylyk@chemistry.leeds.ac.uk.

† Permanent address: Institute for Problems of Materials Science, 3 Krzhyzhanovskogo St., Kiev 03142, Ukraine. E-mail: oom65@yahoo.co.uk.

10.1021/jp0379704 CCC: $27.50
Published on Web 05/11/2004

TABLE 1: Thermal (in °C) and Temporal (in Minutes) Parameters of Heat Treatments Applied to the StOSt Sample

N	quenching	isothermal crystallization	heating	annealing	frames[a]
1	55 °C → 10 °C	10 °C for 60 min	10 °C → 30 °C	30 °C for 10 min	147 × 30 s
2	55 °C → 10 °C	10 °C for 5 min	10 °C → 30 °C	30 °C for 5 min	78 × 30 s
3	55 °C → 0 °C	0 °C for 30 min	0 °C → 30 °C	30 °C for 5 min	78 × 30 s
4	55 °C → 5 °C	5 °C for 30 min	5 °C → 30 °C	30 °C for 5 min	78 × 30 s
5	55 °C → 12.5 °C	12.5 °C for 30 min	12.5 °C → 30 °C	30 °C for 5 min	78 × 30 s
6	55 °C → 12.5 °C	12.5 °C for 1 min	12.5 °C → 30 °C	30 °C for 10 min	86 × 10 s
7	55 °C → 15 °C	15 °C for 30 min	15 °C → 30 °C	30 °C for 5 min	78 × 30 s
8	55 °C → 17.5 °C	17.5 °C for 30 min	17.5 °C → 30 °C	30 °C for 5 min	78 × 30 s
9	55 °C → 20 °C	20 °C for 30 min	20 °C → 30 °C	30 °C for 5 min	78 × 30 s
10	55 °C → 21 °C	21 °C for 30 min	21 °C → 30 °C	30 °C for 5 min	78 × 30 s
11	55 °C → 22.5 °C	22.5 °C for 30 min	22.5 °C → 30 °C	30 °C for 5 min	78 × 30 s
12	55 °C → 10 °C	10 °C for 5 min	10 °C → 30 °C	30 °C for 5 min	28 × 30 s

[a] The number of frames, together with duration of each frame (in seconds) for SAXS/WAXS patterns, are presented in the last column.

possibility to extract information about the position of the glycerol group from the projection of the electron density profile along the layer normal enables the packing arrangements of TAG molecules in the structure to be obtained. The recent application of synchrotron XRD further enhances the capability of this approach in the analysis of the structure of triglycerols, in particular, that of unstable phases formed through a sequence of polymorphic transformations during crystallization.

Well-resolved diffraction peaks of TAG structures can readily be measured at small angles using modern synchrotron or lab-based instruments. Herein, it is demonstrated what kind of structural information on triacylglycerols can be extracted from the intensities of lamellar diffraction peaks. Transformations among structures of 1,3-distearoyl-2-oleoyl-*sn*-glycerol (StOSt) are investigated in detail. This TAG has a particularly rich polymorphism.[14−16]

Experimental Methods

StOSt was investigated as received from Sigma-Aldrich, Inc. without further purification (99.0 wt % found; fatty acid profile: 16:0 palmitic, 0.1%; 18:0 stearic, 66.7%; 18:1 ($n - 9$) oleic, 33.0%; 20:0 icosanoic, trace; minor components, 0.2%; analysis carried out on a capillary column: monoacylglycerol, 0.31%; diacylglycerol, 0.56%; triacylglycerol, 99.13%). X-ray scattering experiments were performed at the Synchrotron Radiation Source, Daresbury Lab, UK, on station 16.1 with a small-angle camera length 1.3 m and $\lambda = 1.41$ Å, where λ is the wavelength of X-ray radiation. A 1D-quadrant detector and a 1D-curved linear detector were used to record SAXS and wide-angle X-ray scattering (WAXS), respectively. Peak positions of wet rat-tail collagen and high-density polyethylene have been used to calibrate small-angle and wide-angle scattering patterns, respectively. SAXS patterns were also corrected for detector response. This operation transforms the recorded diffraction profiles into profiles equivalent to those obtained with a Debye−Scherrer geometry.

The sample was placed in a TA Instruments DSC pan, modified for transmission of X-rays by the insertion of mica windows. The pan was heated and cooled in a modified Linkam THM hot stage.[17] Heating/cooling ramps were performed within the temperature interval 0−55 °C at a rate of 30 °C/min (Table 1). At the beginning of each heating run, the sample was melted at 55 °C for 2 min and then quenched to a defined temperature of isothermal crystallization, followed by rapid heating to 30 °C. SAXS and WAXS data were obtained simultaneously during the thermal treatment. Experiment 12 repeats experiment 2 to check the reproducibility of results after a set of heat treatments. Similar XRD patterns were obtained for both experiments, and no dependence of the crystallization behavior of the sample on the previous heat treatments was observed. The software packages Winplotr,[18] PowderCell for Windows,[19] and CSD[20] have been used both for processing the X-ray powder diffraction patterns and for crystal structure calculations and analysis. The pseudo-Voigt function has been used to fit diffraction maxima.

Modeling of Electron Density Distribution Function. In general, the electron density distribution within a crystal structure at a point (x, y, z) can be expressed as a Fourier series

$$\rho(x,y,z) = \frac{1}{V}\sum_{h=-\infty}^{\infty}\sum_{k=-\infty}^{\infty}\sum_{l=-\infty}^{\infty} F(h,k,l)\, e^{-2\pi i(hx/a + ky/b + lz/c)} \quad (1)$$

where a, b, and c are primitive translations of the lattice, V is the volume of the unit cell, h, k, and l are Miller indices, and $F(h,k,l)$ is a structure factor.[11] For the simplest case of one-dimensional structures (for example, lamellar structures) the series can be rewritten as

$$S(z) = \frac{1}{L}\sum_{l=-\infty}^{\infty} F(l)\, e^{-2\pi i(lz/L)} \quad (2)$$

where L is the period along the layer normal. If the scattering density, $S(z)$, is real everywhere and $F(l)$ and $F(\bar{l})$ are conjugate quantities, the series (2) can be rewritten in the form

$$S(z) = \frac{1}{L}(F(0) + 2S'(z)) \quad (3)$$

where

$$S'(z) = \sum_{l=1}^{\infty} |F(l)| \cos\left(\frac{2\pi lz}{L} - \delta(l)\right) \quad (4)$$

in general and

$$S'(z) = \sum_{l=1}^{\infty} m(l)\,|F(l)| \cos\left(\frac{2\pi lz}{L}\right) \quad (5)$$

is for a structure possessing a symmetry center, a plane of symmetry, or a rotation (screw) axis parallel to the lamellae. The two possible values of the phase angle, $\delta(l)$, in these symmetrical structures (either 0 or π) lead to a positive or negative coefficient (phase sign) $m(l) = F(l)/|F(l)| = \pm 1$ in eq 5.

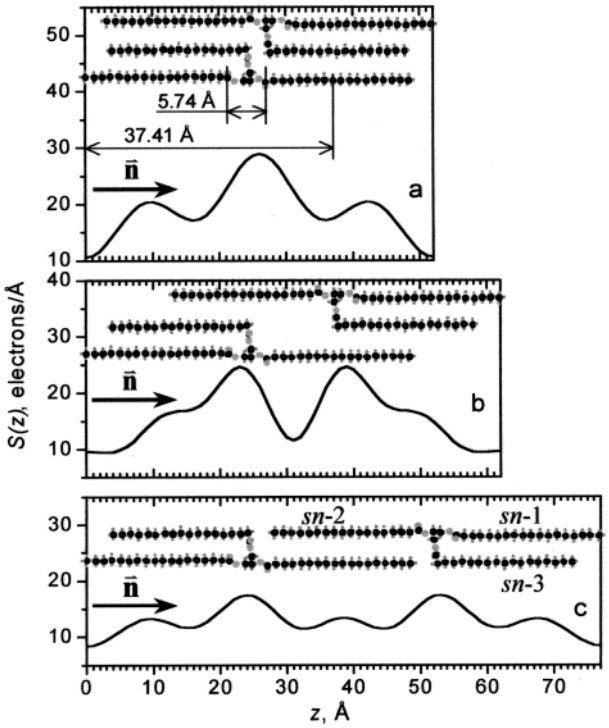

Figure 1. Projection of electron density profile along the layer normal (denoted **n**) calculated for structures in which the separation of tristearin molecules packed in centro-symmetrically related pairs is varied: (a) and (c) represent two-chain ($L = 52$ Å) and three-chain ($L = 77$ Å) packing of the molecules, respectively, and (b) corresponds to an intermediate position ($L = 62$ Å). The distances in part (a) are described in the text. The three stearoyl chains in the tristearin molecule are numbered in part (c) of the figure.

This type of Fourier series has been used effectively to analyze the electron density distribution within lipid bilayers.[12,13] Based on a method developed for solving the structure of the protein hemoglobin,[21,22] the change in intensity of diffraction peaks upon swelling of the lamellar structure as water content increased was used to assign a positive or negative value $m(l)$ to the structure amplitudes, $|F(l)|$. It was demonstrated that a plot of the structure amplitude against distance in reciprocal space lies roughly on a smooth curve, if the signs are suitably chosen (it was also assumed that the structure was symmetrical, see eq 5).[12] As a result, the electron density profile along the bilayer normal was unambiguously derived from these data, and, thus, packing features of lipid molecules within the bilayer, in particular, the distance between lipid headgroups, were determined.

A similar approach can be applied to analyze the crystal structure of triacylglycerols. The TAG molecules are packed in symmetry-related pairs, producing a single-layer arrangement, with the methyl groups and glycerol residues occupying separate regions of the structure.[2] The presence of long hydrocarbon chains packed in a regular, parallel crystallographic array gives rise to X-ray diffraction in two regions. At wide angles, the XRD pattern originates from the subcell structure formed by cross-sectional packing of hydrocarbon chains and is used to identify the three-dimensional relationship between the positions of atoms of a single chain and their lateral neighbors. For example, in a $T_{\parallel}$ subcell structure, all carbons of hydrocarbon zigzag chains belong to planes which are mutually parallel, and in an $O_{\perp}$ subcell structure, all the carbons of a chain belong to a plane which is perpendicular to the planes of its neighbors.[2] The XRD pattern at small angles is associated with the layer packing of triacylglycerol molecules. There is a set of lower-order 00*l* reflections conventionally separated from the general *hkl* reflections, which can be easily identified and indexed in powder diffraction patterns. The positions of these reflections are usually used to determine the period of triacylglycerol layers to obtain a relationship between the lengths of hydrocarbon chains and the layer period, which is generally equal to two (or three) lengths of the acyl chains and is termed a two-chain (or three-chain) layer, respectively. However, to our knowledge, the intensity of these peaks has not been used to reconstruct electron density profiles.

Due to the wide range of structural information accumulated for triacylglycerols,[1,2] especially in the past few years,[9,10] it is possible to demonstrate what kind of data can be extracted from the intensity of the 00*l* reflections. As an example, which in principle leads to general conclusions, the structure of the tristearin (StStSt) molecule, refined recently for the β phase,[10] can be explored for these purposes. This is used as a basis to obtain the electron density profile of the related molecule, StOSt. The relative atomic positions within a single tristearin molecule have been used to model a layer of centro-symmetrically related molecular pairs. To simplify the presentation of the projection of electron density distribution, their hydrocarbon chains have been aligned along the layer normal, with planes of zigzag carbon chains perpendicular to the plane of the figure (Figure 1). Structure factors (and corresponding diffraction intensities), together with phase signs obtained for such a model, can be used to reconstruct the projection of the electron density on the layer normal. Only 00*l* reflections with $q < 0.55$ Å^{-1} ($q = 4\pi \sin\theta/\lambda$, where θ is half of the scattering angle), which is typical for SAXS experiments, have been used in the Fourier series in eq 3 to derive the electron density distribution, $S(z)$. In general, structure factors are expressed as

$$F(h,k,l) = \sum_{j=1}^{n} f_j T_j \, e^{2\pi i(hu_j + kv_j + lw_j)} \qquad (6)$$

where n is the number of atoms in a unit cell and f_j is the scattering factor of atom j whose coordinates u_j, v_j, and w_j are expressed as fractions of the corresponding unit cell dimension. $T_j = e^{-B_j(\sin\theta/\lambda)^2}$ is an isotropic temperature factor where B_j is a Debye−Waller factor. When applied to symmetric lamellar structures (as, for example, in calculating $F(00l)$ for simulated structures of StStSt) the formula (6) can be simplified

$$F(l) = 2\sum_{j=1}^{n/2} f_j T_j \cos 2\pi l w_j \qquad (7)$$

where the summation is only extended to $n/2$, reflecting that the atomic coordinates of only one of the molecules packed in the centro-symmetric molecular pair have to be used. The form (7) was used to obtain structure factors of the simulated StStSt structures. The contribution of the temperature factor is negligible at small diffraction angles (applying Debye−Waller factors reported for the β phase of tristearin,[10] the structure-factor amplitudes are reduced by only 0.7% for the highest 00*l* orders used in the analysis, $q < 0.55$ Å^{-1}), and, thus, $T_j = 1$ was used for all atoms in the TAG molecules.

Several layer structures with intermediate values of long spacing between two-chain and three-chain packings of tristearin molecule (Figure 1a and c, respectively) have been simulated. As might be expected, the highest electron density corresponds to the region associated with the position of glycerol groups

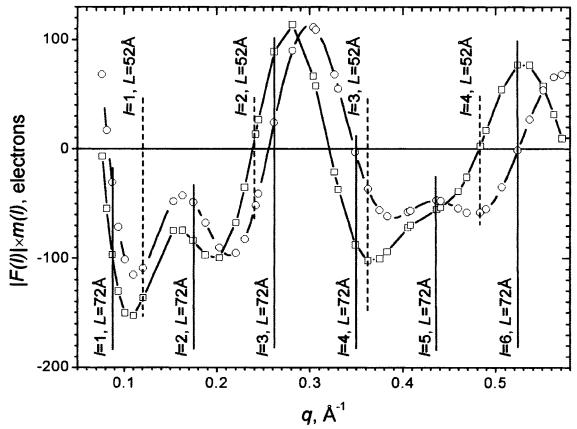

Figure 2. Structure amplitudes, $|F(l)|$, multiplied by phase signs, $m(l)$, versus scattering wave vector, q, for simulated layers of tilted, $\tau = 70°$ (circles), and nontilted (squares) tristearin molecules packed in centro-symmetrically related pairs with different intermolecular separations, as illustrated. Examples of packing of nontilted and tilted molecules are given in Figures 1 and 3, respectively. Positions of structure factors corresponding to lamellar structure with period of layer 52 and 72 Å are indicated on the plot.

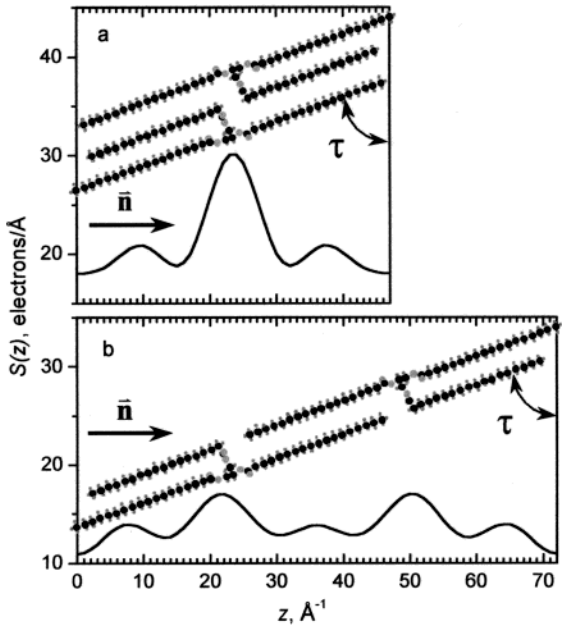

Figure 3. Projection of electron density profile on the layer normal (denoted **n**) calculated for layers of tilted (angle of tilt, $\tau = 70°$) tristearin molecules packed in centro-symmetrically related pairs as illustrated: (a) and (b) represent two-chain ($L = 47$ Å) and three-chain ($L = 72$ Å) packing of the molecules, respectively.

and the bend in a stearoyl chain where the concentration of atoms is greatest. The overlapping projection of glycerol groups (belonging to a pair of StStSt molecules) on the layer normal for the two-chain packing (Figure 1a) generates one strong peak on the electron density profile. The peak splits into two separate peaks following a shift of the molecules (and, therefore, the positions of glycerols) along the layer normal in layers with a longer period (Figure 1b and c). These calculations show that even using truncated Fourier series (not more than seven terms of $|F(l)|$, $l = 0, 1, ..., 6$) produces a reasonable electron density profile, which allows the relative position of glycerol groups within a layer of triacylglycerol molecules to be evaluated.

It has to be noted that the regular structure of the tristearin molecule itself is not changed and is taken to be the same for all the simulated packing structures. The only variable parameter in these calculations is the period of the layer and, thus, the z-axis projection of the relative distance between centers of gravity of the tristearin molecules packed in the centro-symmetric molecular pair. Although, among the simulated structures, only two-chain and three-chain motifs exist in real crystal structures of triacylglycerols, the procedure of continuously changing the distance between molecular centers of gravity includes intermediate packing arrangements of the molecules (Figure 1b), and this illustrates the relationship between structure factors, $F(l)$, corresponding to both two-chain and three-chain layers formed by a particular TAG. In the sense of changing the distance between the centers of gravity of the molecules in a molecular pair (by means of the period of the layer), this simulation is analogous to the change in the spacing of lipid bilayers as a function of water concentration.[12,13] It is noteworthy that structure factors calculated for different layer structures plotted versus q follow a smooth curve (Figure 2, squares), similar to that obtained for lipid bilayers,[12,13] where the intermolecular spacing varies with water content.

TAG molecules crystallized in the most stable crystal form (β phase) usually pack tilted with respect to the basal plane of the layer. For layers formed by tilted molecules (Figure 3), the calculated structure factors again vary smoothly with q (Figure 2, circles). The tilt of the molecules shifts the entire curve of structure factors to higher q values. It is also found that structure factors calculated in the same way for a model of an all-trans regular conformation of StOSt molecules[15] produced a similar curve. This indicates that, for either type of packing (two-chain and three-chain), if the structure of the molecule and its tilt angle are not changed significantly then the structure amplitudes, $|F(l)|$ (at least low orders), multiplied by the corresponding phase signs, $m(l)$, must lie on the same unique curve. The curve shows a sequence of phase signs (positive or negative), which can be used in Fourier series (eq 5) to reproduce the projection of the electron density profile along the layer normal [$S'(z)$]. Thus, the observed two-chain and three-chain packing for some triacylglycerols during polymorphic transformations can be exploited to determine the phase signs of structure amplitudes, $|F(l)|$, and, by means of this, to reconstruct the $S'(z)$.

Experimental Results

The structure of different polymorphs of StOSt has been studied by XRD and analyzed using the method described above.

The applied heat treatment protocols (Table 1) allow at least five polymorphic structures of StOSt to be identified. In every case, after cooling of the sample from the liquid phase to the crystallization temperature, four sharp peaks corresponding to four orders of reflection from a lamellar structure are observed in the SAXS patterns. Depending on the crystallization temperature, the period of the layer, L, is in the range 51.8−54.5 Å (representative diffraction patterns are given in Figures 4 and 5). The appearance of this phase is accompanied by a WAXS peak located at $q = 1.5$ Å^{-1}. Several polymorphs are observed during further isothermal crystallization, carried out at different temperatures. The continuous development of three peaks in the SAXS patterns, corresponding to a lamellar structure characterized by a period $L = 49.1$ Å (a slight temperature dependence is also observed for this parameter), is found at higher temperatures of isothermal crystallization (Figure 4). The SAXS peaks are also accompanied by a WAXS peak corresponding to $d = 4.2$ Å. The layer period obtained for both of these phases may correspond to the two-chain layer motif in

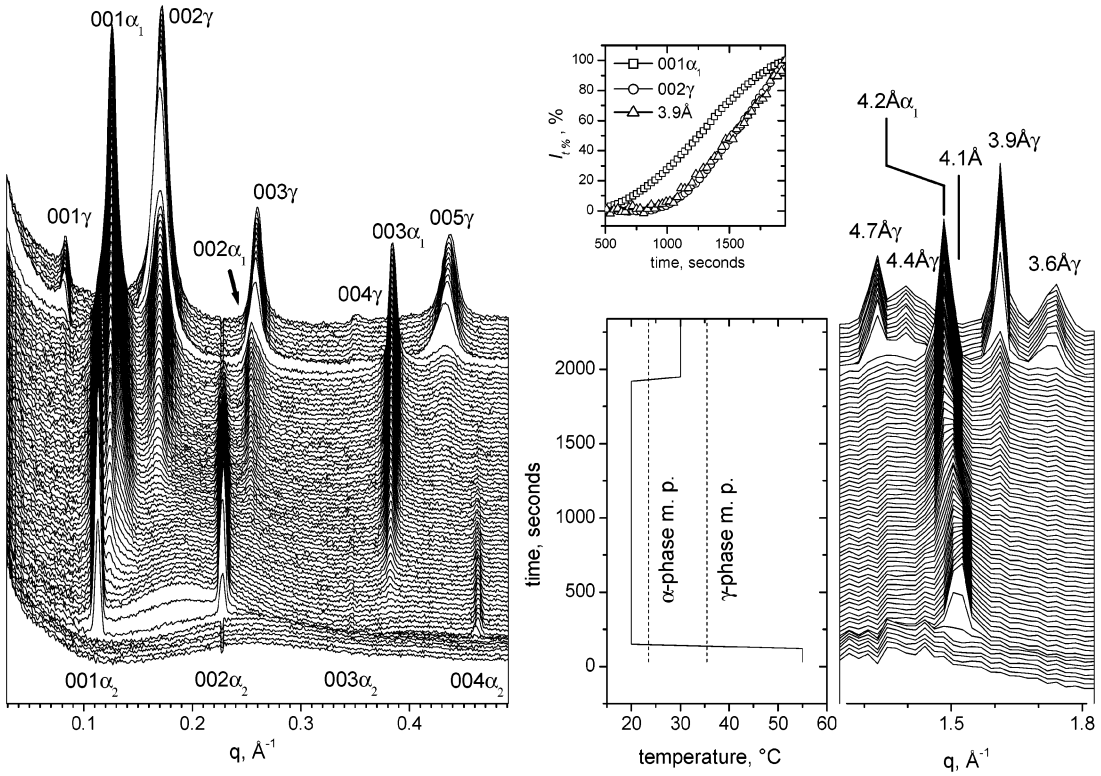

Figure 4. SAXS (left plot, intensity in logarithmic scale) and WAXS (right plot) patterns obtained during isothermal crystallization of StOSt at 20 °C, followed by heating to 30 °C (experiment 9). A diagram showing the temperature profile and melting temperatures (mp) of α and γ phases of StOSt is presented in the central plot. The inset shows the evolution of intensities of small-angle 001_{α_1} and 002_{γ} peaks and wide-angle peak corresponding to *d*-spacing, 3.9 Å, during the isothermal crystallization.

the α phase of StOSt, reported in previous studies ($L = 53$ Å[15] and $L = 48.3$ Å[14]). However, the coexistence of two different phases, which is clearly observed in Figure 4, shows that at least one more phase of StOSt exists. This observation clarifies a significant difference in the layer period of the α phase reported previously.[14,15] In accordance with the classification of glyceride crystal forms,[23] the phase appearing at the beginning of the crystallization of StOSt ($L = 51.8$ Å − 54.5 Å) will be, henceforth, termed α_2, and the more stable phase, appearing later, will be termed α_1. The coexistence of similar polymorphs has been observed in diffraction patterns of cocoa butter,[24] where StOSt is one of the main components.

A coexistence between the α_2 phase and a structure characterized by three broad peaks (peak 1 corresponding to $d_1 \approx 120$ Å; peak 2, $d_2 \approx 40$ Å; and peak 3, $d_3 \approx 16$ Å) is preserved during isothermal crystallization at lower temperatures (Figure 5), and the α_1 phase is not registered under these conditions. Analogous broad peaks ($d_2 = 44$ Å for StOSt[15] and $d_1 = 112$ Å and $d_2 = 36.4$ Å for cocoa butter[24]) have been reported previously; however, there was no clear interpretation. An interpretation of these diffraction patterns is beyond the scope of the current work and will be presented elsewhere. We found that the broad peaks could be produced by a random distribution of two-chain and three-chain packed layers (or domains of these) of StOSt molecules stacked along the layer normal, and it might be identified as a metastable structure. There are two peaks in WAXS also preserved during the isothermal crystallization at lower temperatures (0 and 5 °C). An analysis of the temporal evolution of the normalized intensities, $I_{t\%}$, of these WAXS peaks occurring during isothermal crystallization at 0 °C shows (inset in Figure 5) that the $I_{t\%}$ of the first peak, corresponding to $d = 4.2$ Å, continuously decreases through the crystallization after the appearance of the peak following the slope of the $I_{t\%}$ of the $001_{\alpha 2}$ SAXS reflection (although with an offset in magnitude) and the $I_{t\%}$ of the second peak, corresponding to $d = 3.8$ Å, continuously increases, tracing the most intense SAXS peak, 2, of the metastable structure. This observation indicates that the second peak is related to the metastable structure. Indeed there is no evidence of this peak at higher temperatures of isothermal crystallization, when the metastable structure was virtually absent (Figure 4). The normalized intensities were calculated from $I_{t\%} = (I_t - I_{min})/(I_{max} - I_{min}) \times 100\%$.[24] Herein, I_t is the peak intensity of the diffraction peak, which varies as a function of time, and I_{min} and I_{max} are its minimal and maximal values, respectively.

An increase of temperature to 30 °C (between the melting points of the α and γ phases of StOSt[15]) after isothermal crystallizations leads to significant transformations of the structure of StOSt passing through the melting point of the α_1 phase. Depending on the previous thermal history, the formation of either one series of lamellar peaks (period of layer $L \approx 72$ Å, Figure 4) or two series of lamellar peaks ($L \approx 72$ Å and $L \approx 69$ Å, Figure 5) is observed in the SAXS patterns. The measured periods may correspond to three-chain layers of γ (the longer period) and β' phases.[14,15] WAXS patterns also confirm this identification: a diffraction pattern analogous to that observed for the γ phase reported previously[14] is observed in Figure 4, whereas that presented in Figure 5 can be interpreted as a mixture of two phases (γ and β').

The data in Figure 4 show that the γ phase can be formed by a solid-state transformation from the α_1 phase during isothermal crystallization, carried out at higher temperatures (20−22.5 °C). A weak peak corresponding to $d = 3.9$ Å is simultaneously observed in the WAXS patterns, which could be assigned either to the strongest peak of the γ phase or to the orthorhombicity of the α_1-phase subcell. The temporal evolution of normalized

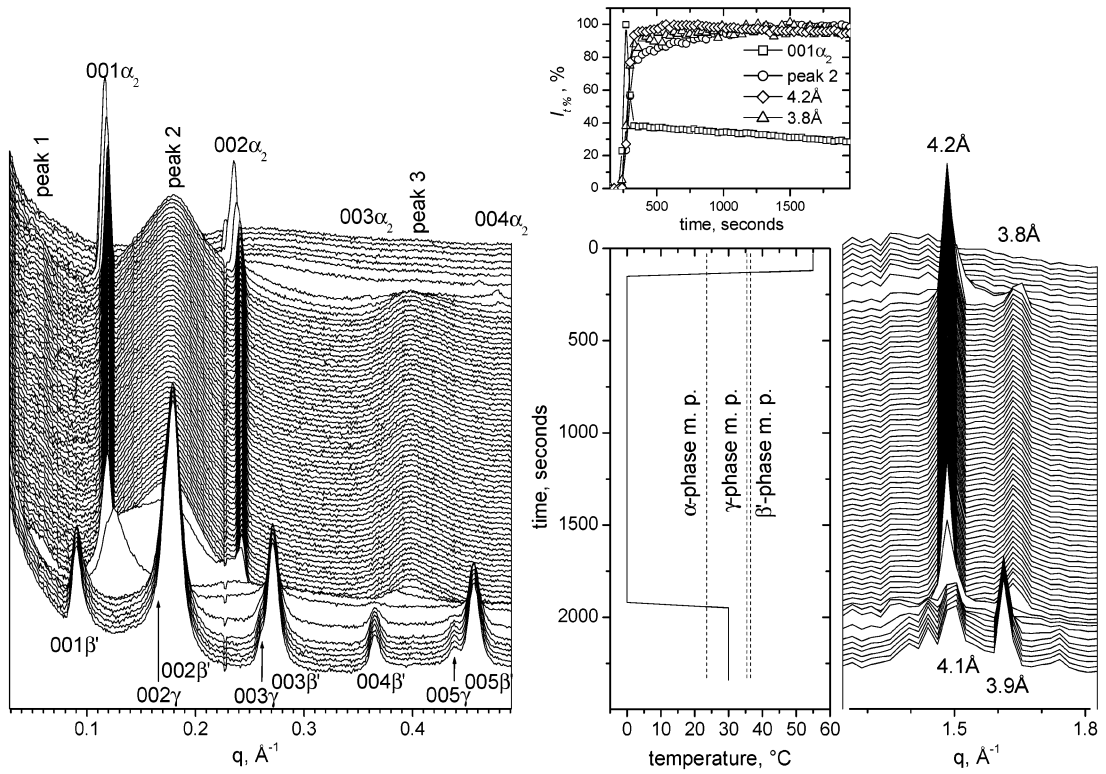

Figure 5. SAXS (left plot, intensity in logarithmic scale) and WAXS (right plot) patterns obtained during isothermal crystallization of StOSt at 0 °C, followed by heating to 30 °C (experiment 3). Broad peaks 1, 2, and 3 are ascribed to a metastable structure of mixed two-chain and three-chain packing of StOSt molecules. A diagram showing the temperature profile and melting temperatures (mp) of α, γ, and β' phases of StOSt is presented in the central plot. The inset shows the evolution of intensities of small-angle peaks labeled 001_{α_2} and peak 2 and wide-angle peaks corresponding to *d*-spacings 4.2 and 3.9 Å during the isothermal crystallization. The order of time frames is reversed in this plot compared to Figure 4 in order to highlight the XRD patterns of the final β' phase.

intensities, $I_{t\%}$, of the peak clearly follows the intensity of the 002γ small-angle peak (inset in Figure 4), indicating that the peak corresponds to the γ phase.

Diffraction data for all mentioned phases, apart from the metastable structure, are summarized in Figure 6 (quantitative information about SAXS data used in the structural analysis is also summarized in Table 2). The patterns containing the most intense peaks, indicating better crystallization of the phases, have been selected. Diffraction data for the as-received sample (before any thermal treatment) are also presented (Figure 6e). Five sharp diffraction maxima in the SAXS pattern, corresponding to a lamellar structure (period of layer $L = 64.5$ Å), are apparent. The origin of a weak sixth peak, assigned fractional Miller indices $00^3/_2$, will be discussed later. The obtained spacing is similar to the period of layer reported for both β_2 and β_1 phases of StOSt[14] ($L = 65$ Å). These phases can be distinguished by WAXS measurements. However, due to the low resolution of the WAXS detector, it was not possible to judge whether a β_2 or a β_1 phase was present. Thus, in a further description, it will be termed simply β phase.

Discussion

Applying the suggested approach, it is desirable to compare the magnitude of structure factors corresponding to different StOSt phases (Table 2). To be able to do so, the observed intensities of all the phases must first be reduced to one scale of intensities. A few assumptions have to be made before the data reduction: (i) there is no change in mass of the sample through the experiments (the sample was sealed in a DSC pan), (ii) the densities of all polymorphs are equal (however, certainly, some differences must exist), (iii) all the sample crystallizes only in the γ phase following melt-mediated crystallization after isothermal crystallization at 20 °C (Table 1, experiment 10; Figure 6c), (iv) all the sample crystallizes either in the α_1 or in the γ phase at the end of applied isothermal crystallization at 20 °C (Table 1, experiment 9; Figure 4; Figure 6b), (v) all the sample crystallizes either in the β' or in the γ phase following melt-mediated crystallization after isothermal crystallization at 0 °C (Table 1, experiment 3; Figure 5; Figure 6d), and (vi) all the phases form a structure characterized by one (or more) of the following symmetry operations: either a symmetry center, a plane of symmetry, or a rotation (or screw) axis parallel to the lamellae, which usually exist in the crystal structure of triacylglycerols.

In accordance with assumption (ii), the weight and volume fractions of the polymorphs presented in the sample are equal. Therefore, the two are not distinguished. Following these assumptions, the 00*l* intensities of three phases (α_1, γ, and β') can be reduced to one scale. The presence of a small amount of γ phase in the sample when crystallized in the α_1 or β' phase (Figure 6b and d, respectively) can be exploited as an internal standard for a calibration to reduce the observed intensities of both phases to one scale. An average value of the ratio of the observed intensities of the three most intense peaks of the γ phase has been used to evaluate the amount of the γ phase (W_γ) in the sample:

$$W_\gamma\,(\%) = \frac{1}{3}\sum_{l=2,\,3,\,5}\frac{I'_{00l}}{I_{00l}} \times 100\% \qquad (8)$$

where I_{00l} are the intensities of the γ-phase peaks when the sample contains 100% of this phase (see assumption (iii)) and

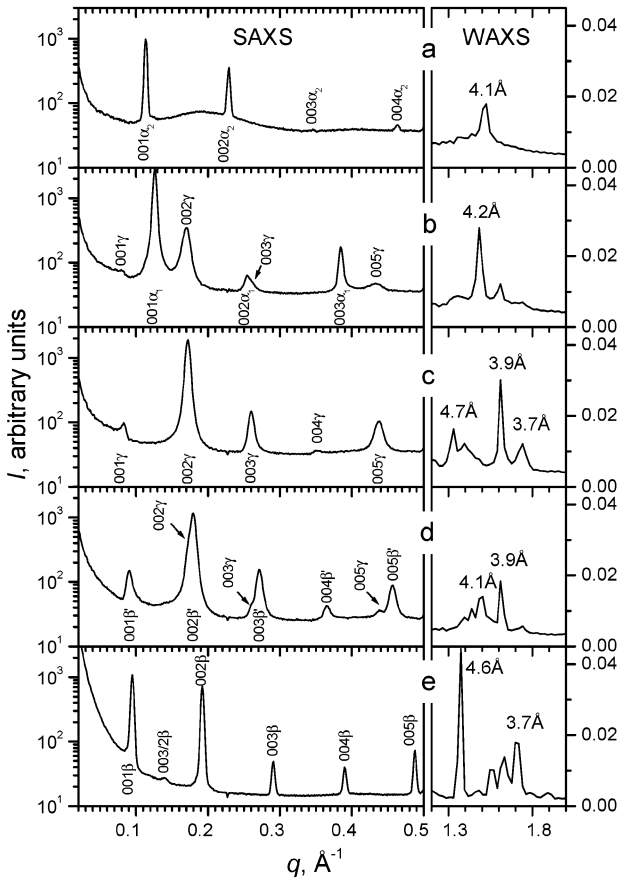

Figure 6. Representative XRD patterns of StOSt phases taken from time-resolved measurements of isothermal crystallization (experiment number, time frame, and temperature at which the patterns were acquired are cited in square brackets after each phase): (a) α_2 phase [experiment 9, frame 13, 20 °C], (b) α_1 phase [experiment 9, frame 67, 20 °C], (c) γ phase [experiment 10, frame 78, 30 °C], (d) β' phase [experiment 3, frame 78, 30 °C], and (e) β phase [as-received sample, 20 °C]. The intensity in the SAXS patterns is shown on a logarithmic scale. Quantitative information extracted from these patterns is summarized in Table 2.

I'_{00l} denotes the intensities of the γ-phase peaks measured in a different crystal state of the sample (see assumptions (iv) and (v)). Subsequently, the amount of either α_1 or β' phase can be obtained by a subtraction (100% $-$ W_γ) and a coefficient for correction of their observed intensities by a ratio (W_γ/100%). The structure amplitudes in these three phases can be calculated afterward from the square root of the intensities divided by the Lorentz-geometrical factor LG $= 1/[(\sin\theta)(\sin 2\theta)]$ (Table 2). The polarization factor proved to be nearly constant at such small angles of diffraction.

At this stage of the investigation, phases, $\delta(l)$ (or, in accordance with assumption (vi), positive or negative signs $m(l) = \pm 1$), can be assigned to all of the obtained structural amplitudes (Table 2, phases α_1, γ, and β') to reconstruct the $S'(z)$. Three nonzero values of structure amplitudes from the measured peaks for the α_1 phase indicate eight possible variants ($=2^3$), and the presence of five peaks for γ and β' phases indicates 32 possible variants ($=2^5$) of assignment for each of the phases. To resolve the problem of the phase assignment, the curves of structure factors obtained for tilted and nontilted tristearin molecules (Figure 2) can be used in further analysis. It has to be noted that only variants where the strongest amplitudes, $|F_{\alpha_1}(001)|$, $|F_\gamma(002)|$, and $|F_{\beta'}(002)|$, were assigned to be negative yield a reasonable projection of electron density profiles, as judged from modeling of the related tristearin molecule (Figures 1 and 3). Using the curves of structure factors establishing the phase sign, $m(l)$, for a particular q value, there is only one consistent assignment for each of these three StOSt phases (Figure 7, open symbols). It appeared that the values of $|F(l)|\,m(l)$ for all three phases lie on a common smooth line, corresponding closely to that calculated for the simulated layers of tristearin molecules (Figure 2).

It is difficult to apply the above approach to reduce the intensity of 00l reflections measured for the other two phases (α_2 and β) onto a common scale. The α_2 phase appears together with a metastable structure, the variable amount of which is problematic to estimate. Although the β phase is observed as a separate phase, there is some uncertainty associated with the assumption that 100% of the as-received sample was crystallized in this particular phase. The high intensity of the forward scattering (Figure 6e), which is a few times higher than that observed after isothermal crystallization (Figure 6a−d), indicates that some amount of the as-received sample was not in a crystalline state. Using the structure-factor curves, the phase signs can be obtained for the structure amplitudes of the α_2 or β phase. Coefficients $m(1) = m(2) = m(4) = -1$ are obtained for the α_2 phase. The q value of the 003_{α_2} reflection corresponds to an area where the curves change their sign from plus to minus; thus, the assignment is ambiguous for this reflection. However, this structure amplitude is very weak and changing the sign does not significantly change the $S'(z)$. Sign "plus" ($m(3) = +1$) was used in the analysis. It must also be noted that among 16 ($=2^4$) possible combinations of assignment, only two of them[25] (derived above) lead to a projection of electron density expected from the modeling. Coefficients $m(1) = m(2) = m(4) = m(5) = -1$ and $m(3) = +1$ may be determined in a similar fashion for the β phase.

Substituting structure amplitudes and their relevant phase signs into eq 5, the projections of electron density profiles along the layer normal $S'(z)$ can be reproduced for each of the phases (Figure 8). Since $F(0)$ was not available from the experiment, only relative variations of the electron density can be determined. Consistent with a layer packing of TAG molecules, a minimum value of $S'(z)$ for all phases is observed at the edge of their layers ($z = nL$, $n = 0, 1, 2, \ldots$). In accordance with assumption (ii), the value of the integral $\int_0^L S(z)\,dz$ has to be constant for all of the phases. Assuming that the minimum value of $S'(0)$ corresponds to zero electron density (since $F(0)$ was not available, this assumption is not fully correct), the integral can be rewritten as $1/L \int_0^L [S'(z) - S'(0)]\,dz$, and correction coefficients ($K_{\alpha 2}$ and K_β) for the α_2 and β phases can be estimated from the relation

$$\frac{K_{\alpha 2}}{L_{\alpha 2}}\int_0^{L_{\alpha 2}}[S'_{\alpha_2}(z) - S'_{\alpha_2}(0)]\,dz = \frac{K_\beta}{L_\beta}\int_0^{L_\beta}[S'_\beta(z) - S'_\beta(0)]\,dz = \frac{1}{L_\gamma}\int_0^{L_\gamma}[S'_\gamma(z) - S'_\gamma(0)]\,dz$$

The amplitudes of the corresponding structure factors can then be placed on a common scale. The corrected structure amplitudes of both phases (α_2 and β) plotted on the graph (Figure 7) are in rather poor agreement with the amplitudes obtained for the other three phases, pointing out that the longitudinal packing of StOSt molecules in these phases has some different features.

All the obtained projections of electron density (Figure 8) are similar to those expected from modeling (Figures 1 and 3). Let us discuss them in the order of appearance of the phases during isothermal crystallizations.

α_2 Phase. This phase appears first in the diffraction patterns after cooling. Although the layer period is close to that for two-

TABLE 2: Miller Indices, *hkl*, Absolute Value of Scattering Wave Vector, *q*, *d*-Spacing, Relative Intensities, *I*, Intensities, I_{obs}, and Corrected Values, I_{cor} (in Arbitrary Units), Amplitudes of Structure Factors, $|F(l)|$ (in Arbitrary Units), and Layer Period, *L*, Obtained for StOSt Phases from Fitting of SAXS Patterns[a]

hkl	*q*, Å^{-1}	*d*, Å	*I*, %	I_{obs}	I_{cor}	$\|F(l)\|$	*hkl*	*q*, Å^{-1}	*d*, Å	*I*, %	I_{obs}	I_{cor}	$\|F(l)\|$
α_2 phase, $L_{\alpha_2} = 54.3(1)$ Å [exp. 9, fr. 13]							β' phase, $L_{\beta'} = 68.9(1)$ Å [exp. 3, fr. 78]						
001	0.113	55.6	100	4.06	12.31	0.063	001	0.090	69.8	10.5	1.17	1.32	0.016
002	0.229	27.4	34	1.39	4.21	0.075	002	0.179	35.1	100	11.16	12.54	0.099
003	0.34	18.5	0.2	0.01	0.03	0.009	003	0.271	23.2	14.3	1.60	1.80	0.057
004	0.463	13.6	1.5	0.06	0.19	0.032	004	0.365	17.2	1.9	0.21	4.70	0.027
α_1 phase, $L_{\alpha_1} = 49.1(1)$ Å [exp. 9, fr. 67]							005	0.457	13.7	7.3	0.82	5.87	0.068
001	0.126	49.9	100	19.23	25.99	0.102	β phase, $L_{\beta} = 64.5(1)$ Å, as received at 20 °C						
002	0.254	24.7	0.6	0.11	0.15	0.015	001	0.095	66.1	100	5.36	7.34	0.041
003	0.385	16.3	5.6	1.08	1.45	0.074	$00^3/_2$	0.140	44.9	0.4	0.02	0.03	0.004
γ phase, $L_{\gamma} = 71.8(2)$ Å [exp. 10, fr. 78]							002	0.192	32.7	65	3.52	4.82	0.067
001	0.084	74.8	2.1	0.35	0.35	0.008	003	0.291	21.6	3.4	0.18	0.25	0.023
002	0.172	36.5	100	16.87	16.87	0.112	004	0.390	16.1	2.8	0.15	0.21	0.028
003	0.260	24.2	7.5	1.26	1.26	0.046	005	0.488	12.9	5.2	0.28	0.38	0.048
004	0.352	17.8	0.2	0.04	0.04	0.012							
005	0.437	14.4	7.2	1.22	1.22	0.077							
006[b]	–	12.0	~0	~0	~0	~0							

[a] The experiment number and time frame used in the fitting are included in square brackets. [b] Information about this reflection was obtained from another experiment; its *d*-spacing was calculated from the value of L_{γ}.

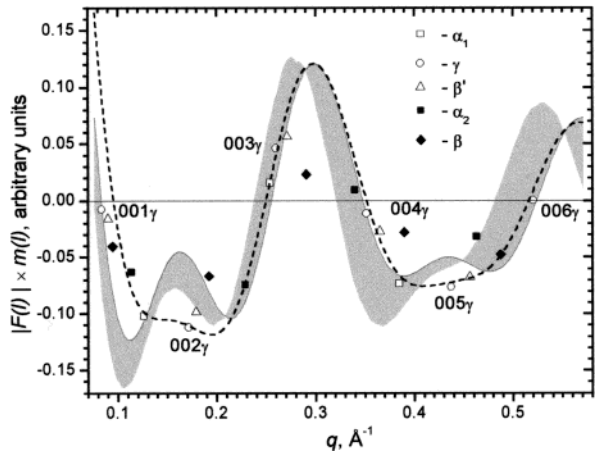

Figure 7. Combined plot of structure amplitudes, $|F(l)|$, obtained for each StOSt phase (Table 2) and multiplied by sign coefficients, $m(l)$, determined in accordance with the curves of structure factors (see Figure 2) versus scattering wave vector, *q*. Structure factors of the γ phase are indexed for convenience. For guidance, the shaded part of the plot corresponds to the area confined by scaled structure-factor curves for simulated layers of tilted and nontilted StStSt molecules. The dashed line corresponds to a scaled structure-factor curve for simulated layers of tilted ($\tau = 70°$) StStSt molecules with reduced occupation of atomic positions of the *sn*-2 chain (the occupation factor was taken to be 0.5). In both cases, the scaling factor was taken as 936.

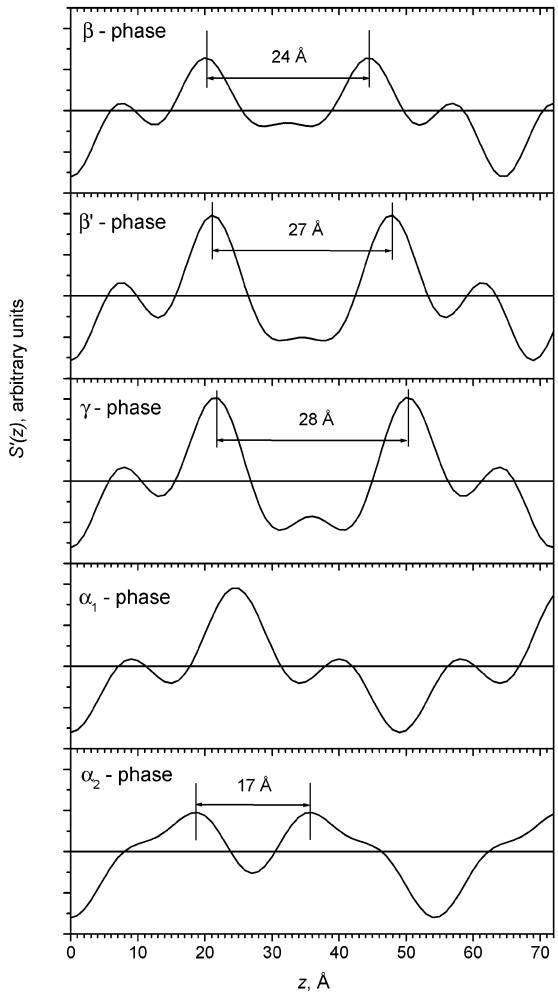

Figure 8. Projection of the electron density profile, $S'(z)$, on the layer normal obtained for StOSt phases by Fourier reconstruction (eq 5), using assigned amplitudes of structure factors presented in Figure 7. The horizontal line indicates $S'(z) = 0$.

chain packing of StOSt molecules, its $S'(z)$ profile is not as expected for two-chain packing (Figure 1a). Instead of one intense peak located at the center of the electron density profile of a single layer, two peaks, well-separated by a distance 17 Å, are observed (Figure 8, α_2 phase). In fact, the observed intensities of diffraction maxima are different from typical diffraction spectra registered for two-chain type packing of TAG molecules. Usually, structures formed by two-chain packing of triacylglycerols are characterized by a very intense first-order peak, a weak (or absent) second-order peak, an intense (or middle) third-order peak, and a weak (or absent) fourth-order peak[26−32] (a similar conclusion can be reached on the basis of calculated XRD patterns, using structural parameters reported for triacylglycerols[3,7,9,10,33]). In contrast, the α_2 phase of StOSt has very intense first- and second-order, vanishingly small third-order, and intense fourth-order peaks (Table 2; Figure 6a). Analysis of SAXS data available in the literature shows that this phase is formed neither by monoacid saturated nor by unsaturated triacylglycerols (for example, tripalmitin (PPP),[30] StStSt,[31] trivaccinin (VVV),[34] trielaidin (EEE),[34] and triolein (OOO)[34]). Also, this phase has not been observed for saturated TAGs consisting of acyl chains with different lengths (for

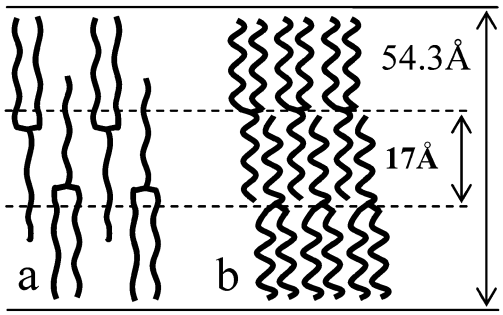

Figure 9. Two possible packing motifs of StOSt molecules in the α_2 phase ((a) and (b)) among which the variant (b) is more favorable. Due to possible random mutual orientation of stearoyl and oleoyl chain within a single molecule,[15] the position of the oleoyl chain is not specified. The figure shows the layer period, L_{α_2}, and the distance between glycerol groups of StOSt molecules obtained from the projected electron density profile (Figure 8).

example, 1,2-dipalmitoyl-3-lauroyl-*sn*-glycerol (PP12),[29] 1,2-dipalmitoyl-3-myristoyl-*sn*-glycerol (PP14),[29] 1,3-dipalmitoyl-2-stearoyl-*sn*-glycerol (PSP),[26] 1,3-distearoyl-2-palmitoyl-*sn*-glycerol (SPS),[26] 1-stearoyl-2,3-dipalmitoyl-*sn*-glycerol (SPP),[26] 1-palmitoyl-2,3-distearoyl-*sn*-glycerol (PSS)[26]). However, this phase can be recognized in diffraction patterns of 1,3-dioleoyl-2-stearoyl-*sn*-glycerol (OSO)[34] and 1,3-distearoyl-2-linoleoyl-*sn*-glycerol (SLS)[35] at the initial stage of crystallization from the melt. Thus, these data suggest that the phase forms only in mixed saturated/unsaturated TAGs, and the presence of both saturated and unsaturated acyl chains in a TAG molecule, which cannot match each other, probably causes the formation of the α_2-phase structure at the beginning of the crystallization.

A set of sharp peaks similar to that observed for the α_2 phase of StOSt was also observed upon quenching melted cocoa butter (where StOSt is one of the main components) from 80 to −10 °C.[24] This set appears together with two broad peaks at 36.4 and 112 Å. It was hypothesised that both sharp peaks and broad peaks correspond to a single form of cocoa butter, where a part of the structure is ordered, while the rest is not. Although a similar coexistence of the sharp and broad peaks is apparent in the diffraction patterns of StOSt at lower isothermal crystallization temperatures (Figure 5), the SAXS patterns recorded at higher temperatures of crystallization are somewhat different (Figure 4): sharp peaks assigned to the α_2 phase are registered through the whole process of isothermal crystallization, while very broad peaks appear briefly only at the beginning of the process. The latter experiment indicates that the sharp and broad peaks are independent, and, therefore, they result from two separate forms of StOSt structures, which may coexist together only under certain thermal conditions of crystallization. In support of this conclusion, sharp peaks similar to those for the α_2 phase were registered in the initial stage of crystallization of SLS, even without any evidence for formation of the other form (i.e., the broad peaks were not observed).[35]

The obtained electron density profile in the α_2 phase (Figure 8) is similar to the profile simulated for the layer of tristearin molecules with glycerols in an intermediate position between two-chain and three-chain layers (Figure 1b). In this proposed structure for the α_2 phase (Figure 9a), there is a significant amount of empty space, which is physically impossible. The most intense peaks in the electron density profile of a TAG molecule are associated with the projection of glycerol groups on the layer normal. Therefore, the distance between glycerol groups in the structure of the α_2 phase is estimated to be 17 Å. Supposing that there is a gap between layers formed by a terrace of methyl groups at the ends of the acyl chains, this separation corresponds to the division of a layer into three nearly equal parts. This suggests three-chain packing of StOSt molecules in the α_2 phase. However, for this type of packing to be consistent with the layer period (L_{α_2} = 54.3 Å, Table 2), the length of each acyl chain would have to be significantly shorter than its length in the all-trans conformation. Packing constraints on the conformational order of the acyl chains at the beginning of crystallization probably lead to a mixed conformation of both stearoyl and oleoyl chains, different from all-trans. Estimations made by using the molecular modeling software Spartan-Pro showed that conformational states of $C_{18:0}$ and $C_{18:1}$ hydrocarbon chains (associated with stearoyl and oleoyl respectively), with axial lengths ca. 17 Å, could be found in which the energy differences relative to the all-trans conformation were small. Thus, it can be expected that at the beginning of crystallization from the liquid phase, the conformational disorder forms an energetically favorable "twisted" structure of acyl chains (Figure 9b). However, a comprehensive computational analysis based on statistical mechanics of chain molecules is required to quantify the conformational order of the entire StOSt molecule. The presence of a WAXS peak at 4.1 Å shows that there is some transverse order in the packing of acyl chains within the α_2-phase layer, which has to be considered in the final model of the phase. The appearance of the WAXS peak (which could be indexed on a hexagonal lattice as a 100 peak corresponding to $q = 4\pi/a\sqrt{3}$, where a is a lateral separation of the acyl chains), together with SAXS peaks corresponding to a periodic lamellar structure (Figure 6a), may allow the α_2 phase to be classified as a smectic B liquid crystal phase;[36] however, to understand the real structure of the α_2 phase, extra experimental information would be required.

It has to be noted that only a portion of the StOSt molecules present in the sample forms the α_2-phase structure at the beginning of crystallization. Another portion of the StOSt molecules organizes in the metastable structure. This effect is probably caused by different pre-ordered states of StOSt molecules coexisting in the liquid phase.

α_1 Phase. The intensities of peaks for the α_1 phase observed in SAXS patterns (Table 2; Figure 6b) are in good agreement with the intensities obtained for a typical two-chain packing of triacylglycerol layers. In particular, there are very intense first-order, weak second-order, and intense third-order peaks. The $S'(z)$ obtained for this phase (Figure 8) is equivalent to one expected for two-chain structure of TAG molecules (Figure 1a or Figure 3a), and there is only one maximum at the layer center. Thus, all glycerol groups of StOSt molecules in the α_1 phase are located within the middle of the layer. In accordance with the relationship between layer period and the total length of acyl chains (expressed by the number of carbon atoms, n) determined for the α form of saturated triacylglycerols,[2] the layer period of a TAG with n = 54 (StStSt) has to be 4.8 Å + (54 Å × 0.85) = 50.7 Å. It is slightly longer than the experimental value obtained for the α_1 phase of StOSt (L_{α_1} = 49.1 Å), but is reasonable if it is considered that the conformational disorder caused by the presence of an unsaturated oleoyl chain can shorten the length of the chain along the chain direction (Figure 10a). Another possible cause for a reduced layer period, tilting of StOSt molecules (Figure 10b), will be discussed later.

γ Phase. The layer period of this phase corresponds to a three-chain packing of StOSt molecules. Unlike the two-chain packing of StOSt molecules, the saturated chains are separated from the unsaturated layers, forming a sequence of sublayers: stearoyl, oleoyl, stearoyl (Figure 11). It has recently been found by IR

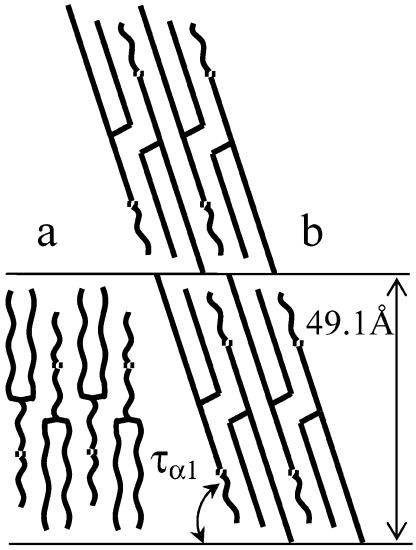

Figure 10. Scale drawing of the packing motif of StOSt molecules in (a) nontilted (perpendicular) and (b) tilted ($\tau_{\alpha_1} = 72.7°$) orientation, with respect to the basal plane of the layer in the α_1 phase. In the tilted variant, one stearoyl chain is assumed to be in an all-trans configuration. The layer period, $L_{\alpha 1}$, is indicated.

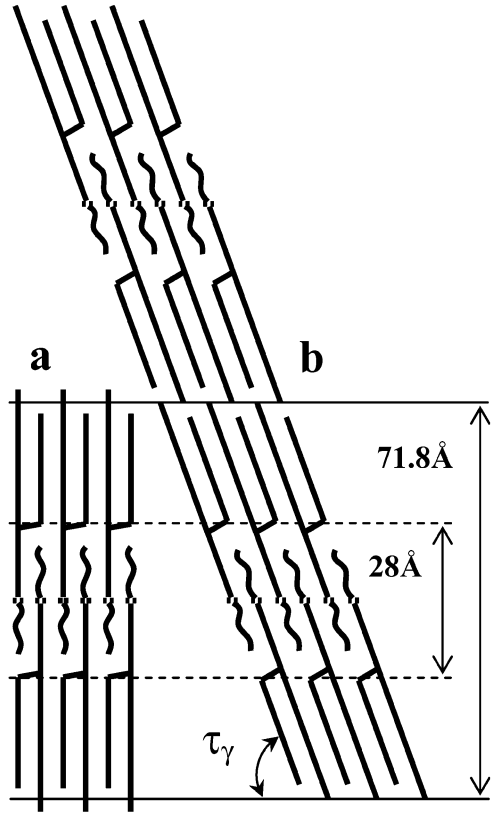

Figure 11. Scale drawing of the packing motif of StOSt molecules in (a) nontilted (perpendicular) and (b) tilted ($\tau_\gamma = 70.5°$) orientation, with respect to the basal plane of the layer in the γ phase. One stearoyl chain is assumed to be in an all-trans configuration. The layer period, L_γ, and the distance between glycerol groups area of StOSt molecules obtained from the electron density profile (Figure 8) are indicated.

spectroscopy[16] that one of the stearoyl chains in StOSt is in a bent conformation in the γ phase, as in the *sn*-3 chain of StStSt; the other stearoyl chain adopts an all-trans conformation and the oleoyl chain is in a disordered state. The $S'(z)$ obtained for this phase from structure amplitudes (Figure 8) is in agreement with that expected from modeling a three-chain structure (Figure 1c or Figure 3b). The two highest electron density peaks correspond to projections of glycerol groups on the layer normal. The corresponding distance is estimated to be 28 Å. The structural motif of the γ phase is usually presented in a manner where the alkyl chain axes are parallel to the layer normal.[14,37] To satisfy the estimated distance in this orientation, it may be assumed that the segments of oleoyl chains between the olefinic group and the glycerol group are in an all-trans conformation and double bonds of centro-symmetrical pairs of the molecules are aligned in the same plane (Figure 11a). However, accepting also the all-trans conformation of one of the stearoyl chains detected by IR spectroscopy, this configuration of StOSt packing produces a longer layer period than the one measured from the SAXS patterns. An estimation based on the geometry of the StStSt molecule crystallized in the β phase[10] shows that the distance between the end carbon of the methyl group of the *sn*-1 chain (stearoyl chain in StOSt) and the middle carbon, 9, of the *sn*-2 chain (carbon of the olefinic group in StOSt) is 37.41 Å (Figure 1a). If all StOSt acyl chains are oriented parallel to the layer normal, then the period of the layer has to be 76.16 Å (=(37.41 Å × 2) + 1.34 Å, where 1.34 Å is the length of the carbon double bond), which is too long in comparison with the measured $L_\gamma = 71.8$ Å (Table 2). Whereas some interpenetration of the end methyl groups of neighboring layers can reduce the calculated value, it is more likely that StOSt molecules are tilted within the layer (Figure 11b). A simple evaluation shows that the tilt angle has to be $\tau_\gamma = \arcsin(71.8/76.16) = 70.5°$ to match the measured L_γ. The angle of the tilt is very close to the theoretical value, $\tau_t = 70°$, calculated for the most favorable packing mode of saturated TAG molecules in three-chain layers with methyl terrace $t = t_1 + t_2 = 1$ ($r = p = 18$, $t_1 = (r - p - 2)/2 = -1$, and $t_2 = 2$; see original work for the notation).[38] Despite the presence of an unsaturated chain (oleoyl) in the StOSt molecule, the measured layer period is in good agreement with the formula for the long spacing L derived for β phases of homologous saturated triacylglycerols with three-chain packing:[38]

$$L = \frac{(n + n_0)}{2} c_s \sin \tau_t \qquad (9)$$

where $n_0 = 6.76$, n is the number of carbon atoms in the acyl chains (=54 for StOSt), and c_s is the subcell period along the acyl chain (2.545 Å[39]). The eq 9 gives a value of 72.65 Å, which is quite close to the experimental value obtained for the γ phase of StOSt. In support of the tilted packing of StOSt molecules, the WAXS pattern of the γ phase contains strong peaks at 4.7, 3.9, and 3.7 Å (Figure 6c) corresponding well to a typical $T_{\parallel}$ subcell (Miller indices 010_s, $1\bar{1}0_s$ and 100_s, respectively) identified for three-chain[27] and two-chain[3,10] packing in β phases of TAGs, with cell parameters $a_s = 4.38$ Å, $b_s = 5.46$ Å, $c_s = 2.545$ Å, $\alpha_s = 71°$, $\beta_s = 110°$, and $\gamma_s = 121°$.[39] The presented analysis demonstrates a good correlation between the structural model derived for triclinic (space group $P\bar{1}$) β phases of saturated TAGs with three-chain packing and the structural parameters measured for the γ phase of StOSt. Relating $T_{\parallel}$ subcell parameters and unit cell parameters derived for three-chain β phases of TAGs,[38] the unit cell parameters of the γ phase of StOSt can be calculated as $a_\gamma = 8.24$ Å, $b_\gamma = 5.46$ Å, $c_\gamma = 78.11$ Å, $\alpha_\gamma = 69.9°$, $\beta_\gamma = 92.3°$, and $\gamma_\gamma = 116.5°$. The evaluated tilt angle, the measured layer period, the identified packing of acyl chains within the layer (most likely $T_{\parallel}$ subcell), and the information on the conformational order of acyl chains of StOSt molecules from IR spectroscopy together create an

essential background for a model of the crystal structure of the γ phase of StOSt.

It has to be noted that the electron density within the middle of the γ-phase layer, associated with a sublayer of the oleoyl chains, is lower than the electron density at the interface of the layer associated with the stearoyl sublayers (Figure 8), which is not expected from modeling (Figure 1c). This effect is probably caused by conformational disorder of the oleoyl chains still remaining in the structure of the γ phase.

It must also be mentioned that, whereas the structure amplitudes of the γ phase $|F_\gamma(001)|$, $|F_\gamma(003)|$, $|F_\gamma(004)|$, and $|F_\gamma(006)|$ follow closely the curve of the structure factors calculated for layers of tristearin molecules tilted at 70° from the layer plane, the structure amplitudes $|F_\gamma(002)|$ and $|F_\gamma(005)|$ show a significant deviation from the curve (Figure 7). The deviations can be caused by the same conformational disorder of the oleoyl chains as discussed above. All three acyl chains in the tristearin molecule used to calculate the curves have an all-trans conformation with well-defined atomic positions. Simulating conformational disorder of the oleoyl chain of StOSt by reducing the occupation of the atomic positions of the *sn*-2 chain of StStSt shows that the pair of double minima of the structure-factor curve observed for negative values, $|F(l)|m(l)$ (Figures 2 and 7), degrades into two single minima suggested by positions of $|F_\gamma(002)|$ and $|F_\gamma(005)|$ in Figure 7, and, moreover, the entire curve passes near all six $|F(l)|m(l)$ values obtained for the γ phase. Thus, the observed deviations of $|F_\gamma(002)|$ and $|F_\gamma(005)|$ from the calculated curve of structure factors for completely conformationally ordered TAG molecules support the results of IR spectroscopy[16] about a conformational disorder of the oleoyl chains of StOSt molecules in the γ phase.

***β* Phase.** Before discussing the β' phase of StOSt, it is preferable to analyze the structure of the β phase of StOSt. A model of the structure of symmetric monounsaturated triacylglycerols (Sat-O-Sat, where Sat is a saturated chain and O is an oleoyl chain) in the β phase has been proposed already.[40] In accordance with the model, the packing motif of StOSt molecule in the β phase is represented in a scale drawing (Figure 12). The stearoyl chains, as well as the saturated parts of the oleoyl chain, are in the all-trans configuration and the carbon double bond area, −C−C═C−C−, has a skew$^+$−cis−skew$^-$-type conformation (this conformation was also suggested later by IR spectroscopy results obtained for the β phase of StOSt[16]). The angle of tilt $\tau_\beta = \tau_{1\beta} = \tau_{2\beta} = 54°$, as found for a methyl terrace $t = -1$.[40]

The measured period of the β-phase layer ($L_\beta = 64.5$ Å) corresponds well to the result, $L = 65.1$ Å, obtained from the equation derived for β phases of homologous unsaturated TAGs with three-chain packing[40]

$$L = (n + n_0)1.03 \text{ Å} \qquad (10)$$

where $n_0 = 9.2$ and the coefficient 1.03 Å originates from $c_s/2 \sin 54°$. The $S'(z)$ (Figure 7) suggests a distance of 24 Å between the positions of projected glycerol groups, which is feasible considering the model proposed earlier[40] (Figures 12 and 13a).

Applying the approach described previously, the curve of structure factors can be calculated for simulated layers of StStSt molecules tilted with respect to the basal plane of the layer at the predicted angle $\tau_\beta = 54°$. Only one coordinate describing the position of the atoms along the layer normal is used in the calculations. Thus, a symmetry-related molecular pair of StStSt molecules can, in general, reproduce the projection of StOSt atomic positions on the layer normal (the latter being represented

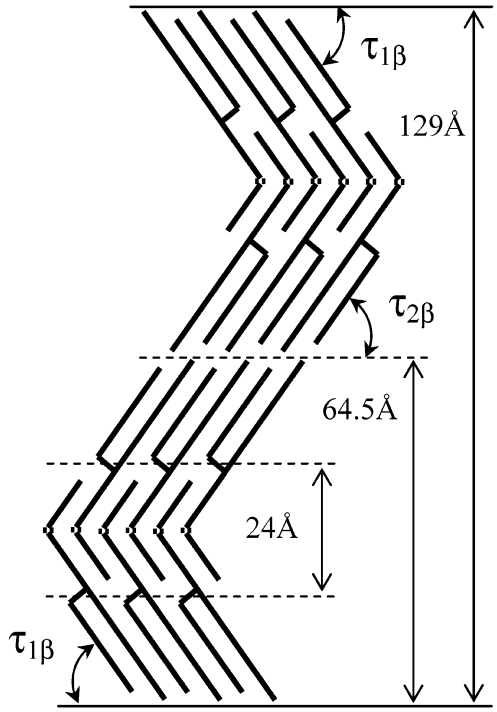

Figure 12. Scale drawing of the packing motif of StOSt molecules in the β phase[40] ($\tau_{1\beta} = \tau_{2\beta} = 54°$). Figures show layer period, $2L_\beta$ (six-chain length), half a period of the layer, L_β (three-chain length), and the distance between glycerol groups of StOSt molecules obtained from the electron density profile (see Figure 8).

in Figure 13a). A pair of StStSt molecules related either by mirror (glide) plane (Figure 13b) or by a center of inversion (Figure 13c) will produce the same result in the calculations. One comment has to be made before discussing the calculation. In accordance with formulas derived for the long spacing, L, of triclinic β phases of homologous saturated TAGs with two-chain[39] or three-chain packing (see eq 9), the coefficient associated with the non-subcell area of the crystal structure (glycerols and methyl terrace bounding the layer) is given by $n_0 = 6.62$ and 6.76, respectively. Accepting that the tilt angle $\tau = 90°$, the coefficient expressed in angstrom units is 5.62 and 8.60 Å, respectively. The obtained values are equivalent[41] to a distance of 5.74 Å measured in StStSt molecule between projections of carbon atoms of *sn*-1 and *sn*-2 chains esterified to glycerol (Figure 1a). Therefore, the coefficient, n_0, obtained for β phases of saturated TAGs is totally related to glycerol geometry, and there is no contribution to this coefficient from methyl terraces. Thus, this evaluation suggests that all methyl group carbon atoms of *sn*-1 chains of saturated TAGs crystallized in triclinic β phase have either to belong or to be located quite close to interlayer planes. This consideration has been taken into account in the simulation of layers of tristearin molecules to calculate the structure-factor curve (Figures 1 and 3). Meanwhile eq 10, derived for the long spacing, L, of three-chain layer of β phases of Sat-O-Sat, contains a larger coefficient ($n_0 = 9.2$), indicating that some contribution from the methyl terrace (and probably also from the carbon double bond) is present. Thus, this fact has to be considered when simulating the layer structure of StStSt to model the β-phase packing of StOSt. Following the above evaluation, the methyl group carbon atoms of *sn*-1 chains of StStSt (and, therefore, the entire molecule) have to be shifted along the layer normal by 1.26 Å ($= [(9.2 - 6.76)/2] \times 1.03$ Å) from the interlayer planes (Figure 13). Curves of structure factors of layers of tilted StStSt molecules calculated for both nonshifted and shifted methyl

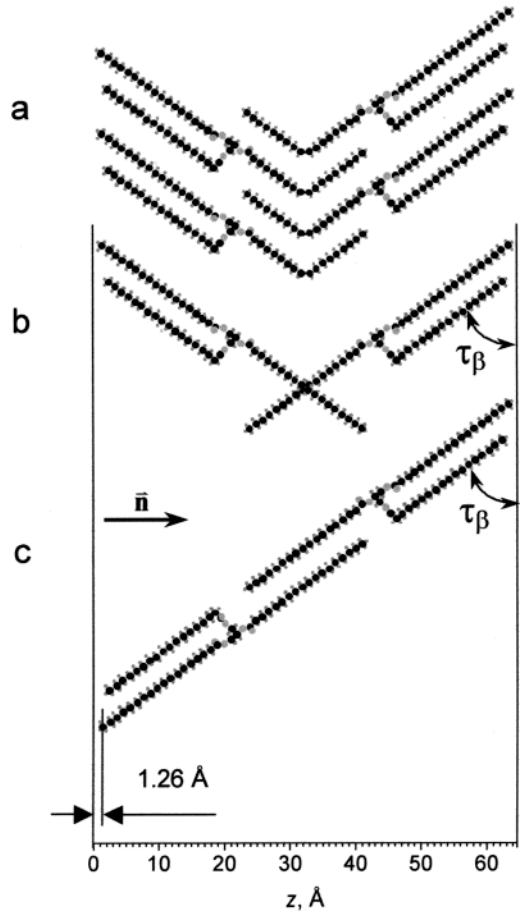

Figure 13. Packing of StOSt molecules in the β phase (a) and a mutual orientation of symmetrically related pairs of StStSt molecules ((b), for mirror plane-related and (c), centro-symmetrically related), giving atomic positions of StOSt molecules packed in the β-phase layer used to calculate curves of structure factors presented on the next figure ($\tau_\beta = 54°$). The origin of the gap, 1.26 Å, between the methyl group carbon of the *sn*-1 chain of StStSt and interlayer plane is discussed in the text. The direction of the layer normal is denoted.

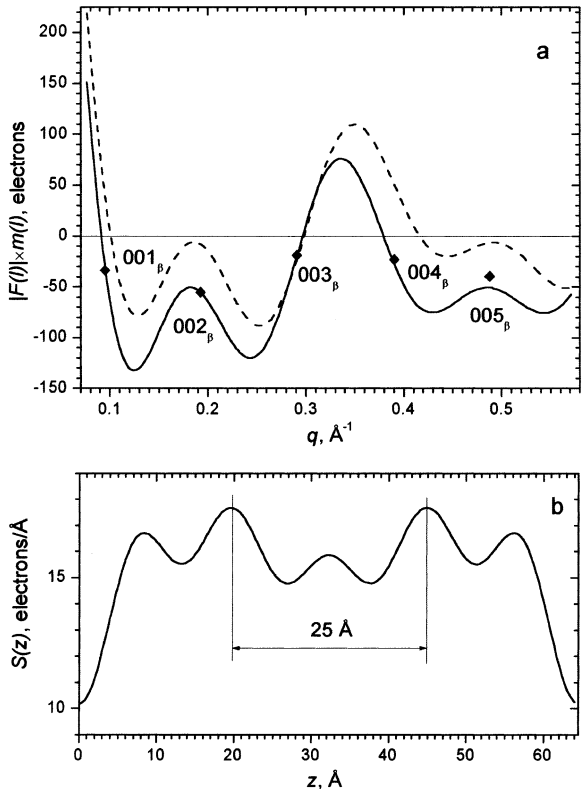

Figure 14. (a) Curves of structure amplitudes, $|F(l)|$, multiplied by phase signs, $m(l)$, versus the scattering wave vector, q, for simulated layers of tilted ($\tau = 54°$) tristearin molecules packed in centro-symmetrically related pairs with different arrangements. The solid line corresponds to the simulated layer of tristearin molecules packed with a gap of 1.26 Å between the methyl group carbon in the *sn*-1 chain of StStSt and the interlayer plane, and the dashed line corresponds to the packing of the molecules without the gap. Diamond symbols show β-phase amplitudes of structure factors (Table 2) reduced to the scale of the calculated curves. The scaling factor 820, giving the best fit to the solid curve, was used for the reduction. (b) $S(z)$ obtained for the β phase of StOSt by Fourier reconstruction (eq 3), using assigned amplitudes of structure factors presented in part (a) of the figure. $F(0) = 996$ (equal to the number of electrons in a pair of StOSt molecules).

group carbons demonstrate features similar to the previous curves (compare Figures 14a and 2). It is revealed that all structure amplitudes of the β phase of StOSt reduced by the scaling factor and assigned a negative phase sign ($m(l) = -1$, $l = 1, 2, ..., 5$) fit the curve of the structure factor obtained for layers of shifted StStSt molecules. A slight deviation observed for $|F_\beta(005)|m_\beta(005)$ may originate from thermal vibrations, which are not accounted for in the calculations. Thus, the obtained results confirm the model developed for packing of Sat-O-Sat molecules in the β phase.[40] The significant deviations of $|F_\beta(l)|m_\beta(l)$ from curves of structure factors observed previously (Figure 7) are caused by the smaller tilt angle of molecules, 54°. Whereas phase signs obtained previously have to be corrected in accordance with the new assignment ($m_\beta(004)$ must be taken as negative), the re-evaluated projection of electron density profile along the layer normal for the β phase of StOSt shows similar features (compare Figures 14b and 8) with a distance of 25 Å between the most intense peaks, corresponding to glycerol groups.

Unlike the γ-phase layer, the electron density within the middle of the β-phase layer, associated with the sublayer of oleoyl chains, and the electron density at the interface of the layer, associated with the stearoyl sublayers, are relatively similar (Figure 14b), as expected from the modeling (Figure 1c or 3b). This fact confirms the conformational order of the oleoyl chains within the crystal structure of the β phase.

Diffraction patterns of the β phase of StOSt contain a weak reflection at $q = 0.14$ Å^{-1} ($d = 44.8$ Å) (Table 2, Figure 6), observed also in a previous work.[42] Using the measured period of the layer (64.5 Å), it may be assigned by fractional Miller indices $00^3/_2$ (Table 2), suggesting an increase of the period by a factor of 2. The total period of the β-phase layer expected from the model[40] has to be 129 Å (Figure 12), and the layer corresponds to six-chain packing, as suggested previously.[42] Due to the assumed symmetry of the model structure (glide planes at the double bonds and inversion centers between the methyl groups), 00*l* reflections with odd *l* must have zero intensity, and only the reflections with even *l* are observed in the diffraction pattern, leading to an apparent three-chain packing. The fact that both parts of each molecule are equally tilted ($\tau_{1\beta} = \tau_{2\beta}$) causes the glide-plane symmetry. A slight difference in the tilt angles, $\tau_{1\beta}$ and $\tau_{2\beta}$ ($\tau_{1\beta} \neq \tau_{2\beta}$), breaks this operation of symmetry, making 00*l* reflections with odd *l* nonzero. Thus, it is most likely that slight distortions of the ideal symmetrical model, which are expected in the real structure of unsaturated TAGs, can cause the appearance of 00*l* reflections with odd *l* (in particular, 003), evidencing six-chain packing of StOSt molecules in the β phase. Packing in a six-chain layer has also

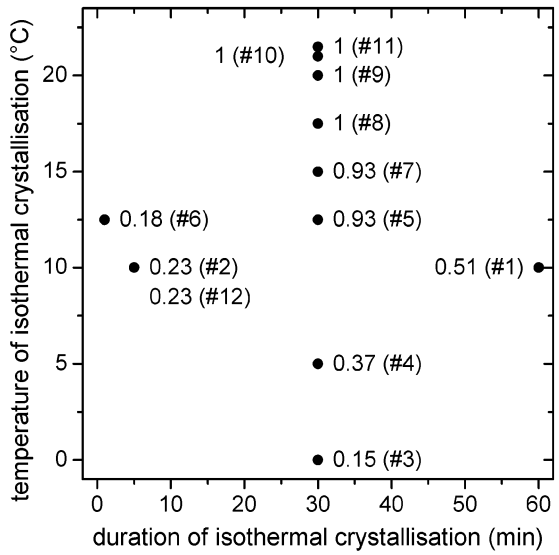

Figure 15. Relative amount of γ phase crystallized in StOSt at 30 °C following isothermal crystallization at the temperatures and for the periods indicated. Each dot represents one of the experiments listed in Table 1 (the number of the experiment is given in brackets).

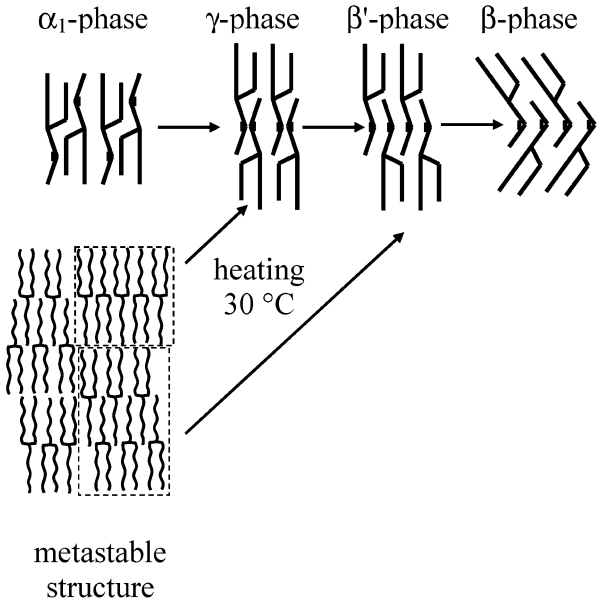

Figure 16. Schematic pathway of polymorphic transformations occurring in the structure of StOSt during crystallization processes. The metastable structure is presented as coexisting domains of two-chain and three-chain packing of StOSt molecules (shown in the dashed rectangles).

been reported for other mixed saturated/unsaturated TAGs (1,3-palmitoyl-2-oleoyl-*sn*-glycerol (POP),[42] 1,3-myristoyl-2-oleoyl-*sn*-glycerol (MOM),[42] 1,2-myristoyl-3-oleoyl-*sn*-glycerol (OOM),[43] and 1,2-palmitoyl-3-oleoyl-*sn*-glycerol (OOP)[43]), where the 003 peak was the most intense one among 00*l* reflections with odd *l*, and, in addition, even a weak first-order peak was observed.[43]

However, another interpretation of the spacing distance, $d = 44.8$ Å, may exist. Due to a small amount of tristearin which might be present in the sample (<0.2 wt %), the observed peak can be attributed to the most intense 001 reflection from the β phase of tristearin, as revealed in cocoa butter.[24]

***β′* Phase.** The layer period of this phase ($L_{\beta'} = 68.9$ Å) corresponding to three-chain packing of StOSt molecules is slightly less than the period of the γ phase. As in the case of the γ phase, it was concluded from IR spectroscopy[16] that one of the stearoyl chains adopts a bent conformation, the other stearoyl chain is in the all-trans form, and the oleoyl chain is in a disordered state. The $S'(z)$ of this phase is similar to that for the γ phase (Figure 8), with a slightly smaller distance between projections of glycerol positions (27 Å).

Performing isothermal crystallization of the α phases at different temperatures within the interval 0−22.5 °C (Table 1), it is found that the competitive formation of more stable γ and β' phases of StOSt during later heating/annealing at 30 °C depends on products formed during the prior isothermal crystallization. Pure γ phase (without β' phase) was detected in SAXS/WAXS patterns only after the α_1 phase was clearly formed during the isothermal crystallization (compare Figures 4 and 5). In this case, the γ phase appeared even during the process of isothermal crystallization of the α_1 phase (for example, Figure 4) starting at a temperature of 17.5 °C, which is lower than the melting point of the α phase (23.5 °C[14]), indicating a transition of the α_1 phase into the γ phase in a premelted state. In contrast, pure β' phase is not formed following any of the presented treatments (Table 1). However, it is found that its formation at 30 °C is favored by a shorter period of isothermal crystallization and/or lower temperatures of isothermal crystallization (Figure 15), when the metastable structure is predominant (Figure 5).

These observations, together with the main structural features derived for the α_1 phase, the γ phase, and the model hypothesized for the metastable structure, suggest the following schematic pathway of transformations (Figure 16) among StOSt structures. The premelting transition of the α_1 phase into the γ phase indicates affinity of packing of StOSt molecules in these two phases. TAG molecules adopt a chairlike shape in the crystal state, usually forming a two-chain arrangement of pairs of centro-symmetrically related molecules with their bent acyl chains oriented virtually in opposite directions. Probably, StOSt molecules tend to adopt this packing motif in the α_1 phase. A similar opposite orientation of the bent chains is found in the γ phase (Figure 11). The three-chain packing of StOSt in the γ phase can be obtained from the two-chain packing in the α_1 phase by a shift of the molecules parallel to the axis of acyl chains[44] (Figure 16). Thus, there are no structural restrictions on the formation of the γ phase, either from a premelted state or from melted state of the α_1 phase, observed in the experiments. The driving force for this transformation is the lateral separation of incompatible monounsaturated oleoyl and saturated stearoyl chains into different sublayers.

Four different symmetric arrangements of pairs of TAG molecules are conceivable in three-chain packing mode.[38] These arrangements produce two variants of mutual orientation of bent acyl chains. The first one (an opposite direction of the bent acyl chains), associated with a center of symmetry or a 2-fold rotation axis normal to the molecular plane, occurs in the γ phase of StOSt (Figure 11), and the second one (an along direction of the bent acyl chains), associated with a 2-fold screw axis lying in the molecular plane at right angles to the chain axes or a glide plane perpendicular to the chain axes, is recognizable in the structure of the β phase of StOSt (Figure 12). Because the skew$^+$−cis−skew$^-$ conformation of the oleoyl chain is compatible with the glide-plane symmetry, the second variant is structurally favorable for StOSt molecules. To adopt the second variant, existing in the most stable β phase, the conformation of the glycerol groups in half the StOSt molecules in the γ phase has to change into a mirror-symmetrical one. Thus, it may be assumed that the β' phase is a crystal structure of StOSt

molecules stabilized after reorientation of the bent acyl chains of the molecular pairs from mutually opposite direction into a common direction (Figure 16).

There are two experimental facts in support of this assumption. First, crystallization of the β' phase at 30 °C does not occur directly after melting the α_1 phase (Figure 4). StOSt molecules in the two-chain arrangement of the α_1 phase cannot adopt directly the common direction of the bent acyl chains proposed in the β' phase and have to be shifted first into three-chain packing in the γ phase: a transformation facilitated through thermal energy transfer. However, the β' phase crystallizes preferentially at the same temperature (30 °C) after melting of the metastable structure (Figure 5), which is supposed to contain a mixture of two-chain and three-chain packing of StOSt molecules. The StOSt molecules in the three-chain packing motif are already prearranged to adopt the more favorable common direction of the bent acyl chains, and the direct formation of the β'-phase structure occurs without passing through the γ phase. The remainder of the StOSt molecules (in the two-chain packing) of the metastable structure tend to adopt the three-chain packing of the γ phase first, as already discussed. Thus, a mixture of two phases (γ and β') is observed in diffraction patterns after melting of the metastable structure. The amount of each phase is rather controlled by the number of two-chain and three-chain pairs of StOSt molecules packed in the metastable structure.

At the final stage of the transformation, when StOSt molecules are arranged in the structure of the β' phase, heat induces conformational ordering of the oleoyl chains so that they can adopt the most stable β-phase configuration (Figure 16).

As in the γ phase, all five terms, $|F_{\beta'}(l)|m_{\beta'}(l)$, obtained for the β' phase follow the curve of structure factors calculated for tilted StStSt molecules with weakened atomic positions of the *sn*-2 chain. This observation, together with the reduced electron density in the mid-plane of the layer, supports results from IR spectroscopy,[16] indicating conformational disorder of the oleoyl chains of StOSt molecules in the structure of the β' phase.

Concluding Remarks

The simulated packing of tristearin molecules in lamellar structures used in this study to model the projection of the electron density profile along the layer normal allows a relationship between structure amplitudes and their phase signs to be obtained. It has been shown that the relationship can be successfully used in Fourier reconstruction of the projected electron density profile of 1,3-distearoyl-2-oleoyl-*sn*-glycerol crystal phases from the intensities of the first few 00*l* peaks recorded in SAXS profiles. This approach can be applied for other triacylglycerols packed in lamellar-like structures, including TAG molecules comprised of acyl chains with a different number of carbon atoms. To avoid an incorrect assignment of phase signs to structure amplitudes, a great deal of attention has to be paid to two parameters in the simulation of the TAG layers: the angle of tilt of acyl chains with respect to the basal plane of the layers and the distance between terminal methyl group carbon atoms and the basal plane of the layer.

It is concluded that six phases (α_2, α_1, γ, β', β_2, and β_1) and one metastable structure can be formed by StOSt molecules in the solid state. Two α phases have been distinguished in this study. Although the layer period of the α_2 phase forming during the initial stage of StOSt crystallization is close to that expected for two-chain packing of StOSt molecules, this phase has a projection of the electron density profile along the layer normal intermediate between that determined for two-chain and three-chain packing of TAG molecules. It is found that this phase can be formed only by mixed saturated/unsaturated TAGs. The structure of the α_2 phase suggested in this study, i.e., three-chain packing of StOSt molecules with twisted acyl chains produced by conformational disorder of the chains, needs further investigation by other time-resolved structural techniques.

The projection of the electron density profile along the layer normal obtained for crystal phases of TAGs (in particular, γ, β', and β phases of StOSt) formed by three-chain packing of the molecules confirms the packing suggested previously only on the basis of the layer period. The structural parameters of the γ phase and the β phase determined in this study and structural models based on this are compatible with a terrace-like arrangement of the terminal methyl group of acyl chains built by de Jong et al.[38,40] Lattice parameters of the γ phase of StOSt are estimated from the model.

Acknowledgment. O.O.M. is grateful to the University of Leeds for the Visiting Fellowship. This work was also supported by EPSRC grant GR/N22052 to I.W.H. The authors thank Prof. Malcolm J. W. Povey for chemical analysis. The authors also thank the SRS, Daresbury Lab for beamtime for the SAXS/WAXS experiments.

References and Notes

(1) *Crystallization Processes in Fats and Lipid Systems*; Sato, K., Garti, N., Eds.; Marcel Dekker: New York, 2001; p 533.
(2) Small, D. M. *The Physical Chemistry of Lipids*; Plenum Press: New York, 1986.
(3) Vand, V.; Bell, I. P. *Acta Crystallogr.* **1951**, *4*, 465.
(4) Jensen, L. H.; Mabis, A. J. *Acta Crystallogr.* **1966**, *21*, 770.
(5) Doyne, T. H.; Gordon, J. T. *J. Am. Oil Chem. Soc.* **1968**, *45*, 333.
(6) Goto, M.; Kodali, D. R.; Small, D. M.; Honda, K.; Kozawa, K.; Uchida, T. *Proc. Natl. Acad. Sci. U.S.A.* **1992**, *89*, 8083.
(7) van Langevelde, A.; Van Malssen, K.; Hollander, F.; Peschar, R.; Schenk, H. *Acta Crystallogr.* **1999**, *55*, 144.
(8) Culot, C.; Norberg, B.; Evrard, G.; Durant, F. *Acta Crystallogr., Sect. B: Struct. Sci.* **2000**, *56*, 317.
(9) Van Langevelde, A.; Van Malssen, K.; Driessen, R.; Goubitz, K.; Hollander, F.; Peschar, R.; Zwart, P.; Schenk, H. *Acta Crystallogr., Sect. B: Struct. Sci.* **2000**, *56*, 1103.
(10) van Langevelde, A.; Peschar, R.; Schenk, H. *Acta Crystallogr., Sect. B: Struct. Sci.* **2001**, *57*, 372.
(11) James, R. W. The Optical Principles of Diffraction of X-rays. In *The Crystalline State*; Bragg, L., Ed.; Cornell University Press: New York, 1965; p 342.
(12) Torbet, J.; Wilkins, M. H. F. *J. Theor. Biol.* **1976**, *62*, 447.
(13) Tristram-Nagle, S.; Liu, Y. F.; Legleiter, J.; Nagle, J. F. *Biophys. J.* **2002**, *83*, 3324.
(14) Sato, K.; Arishima, T.; Wang, Z. H.; Ojima, K.; Sagi, N.; Mori, H. *J. Am. Oil Chem. Soc.* **1989**, *66*, 664.
(15) Ueno, S.; Minato, A.; Seto, H.; Amemiya, Y.; Sato, K. *J. Phys. Chem. B* **1997**, *101*, 6847.
(16) Yano, J.; Sato, K.; Kaneko, F.; Small, D. M.; Kodali, D. R. *J. Lipid Res.* **1999**, *40*, 140.
(17) Bras, W.; Derbyshire, G. E.; Devine, A.; Clark, S. M.; Cooke, J.; Komanschek, B. E.; Ryan, A. J. *J. Appl. Crystallogr.* **1995**, *28*, 26.
(18) Roisnel, T.; Rodriguez-Carvajal, J. WinPLOTR: A Windows tool for powder diffraction pattern analysis. In *Epdic 7: European Powder Diffraction, Parts 1 and 2*; Trans Tech Publications Ltd.: Zurich-Uetikon, 2001; Vol. 378-3, p 118.
(19) Nolze, G.; Kraus, W. *Powder Diffr.* **1998**, *13*, 256.
(20) Akselrud, L. G.; Grin, Y. N.; Zavalij, P. Y.; Pecharsky, V. K.; Fundamenskii, V. S. CSD—Universal program package for single crystal and/or powder structure data treatment; 12th European crystallographic meeting, Moscow, USSR, 1989.
(21) Bragg, L.; Perutz, M. F. *Proc. R. Soc. London, Ser. A* **1952**, *213*, 425.
(22) Perutz, M. F. *Proc. R. Soc. London, Ser. A* **1954**, *225*, 264.
(23) Larsson, K. *Acta Chem. Scand.* **1966**, *20*, 2255.
(24) Loisel, C.; Keller, G.; Lecq, G.; Bourgaux, C.; Ollivon, M. *J. Am. Oil Chem. Soc.* **1998**, *75*, 425.
(25) Two other combinations exist ($m(l) = 1, -1, -1, -1$ and $m(l) = 1, -1, 1, -1$); however, they produce the same projection of electron density

on the layer normal as the other two ($m(l) = -1, -1, 1, -1$ and $m(l) = -1, -1, -1, -1$, respectively), with the only difference being that it is shifted by half a period of layer ($S'_{1,-1,-1,-1}(z + L_{a_2}/2) = S'_{-1,-1,1,-1}(z)$).

(26) Lutton, E. S.; Jackson, F. L.; Quimby, O. T. *J. Am. Chem. Soc.* **1948**, *70*, 2441.

(27) Jackson, F. L.; Lutton, E. L. *J. Am. Chem. Soc.* **1949**, *71*, 1976.

(28) Kodali, D. R.; Atkinson, D.; Redgrave, T. G.; Small, D. M. *J. Am. Oil Chem. Soc.* **1984**, *61*, 1078.

(29) Kodali, D. R.; Atkinson, D.; Small, D. M. *J. Lipid Res.* **1990**, *31*, 1853.

(30) Kellens, M.; Meeussen, W.; Gehrke, R.; Reynaers, H. *Chem. Phys. Lipids* **1991**, *58*, 131.

(31) Lavigne, F.; Bourgaux, C.; Ollivon, M. *J. Phys. IV* **1993**, *3*, 137.

(32) Yano, J.; Kaneko, F.; Kobayashi, M.; Kodali, D. R.; Small, D. M.; Sato, K. *J. Phys. Chem. B* **1997**, *101*, 8120.

(33) Helmholdt, R. B.; Peschar, R.; Schenk, H. *Acta Crystallogr., Sect. B: Struct. Sci.* **2002**, *58*, 134.

(34) Kodali, D. R.; Atkinson, D.; Redgrave, T. G.; Small, D. M. *J. Lipid Res.* **1987**, *28*, 403.

(35) Takeuchi, M.; Ueno, S.; Yano, J.; Floter, E.; Sato, K. *J. Am. Oil Chem. Soc.* **2000**, *77*, 1243.

(36) Seddon, J. M. Structural Studies of Liquid Crystals by X-ray Diffraction. In *Handbook of Liquid Crystals*; Vill, V., Ed.; Wiley-VCH: Weinheim, 1998; Vol. 1, p 635.

(37) Kaneko, F.; Yano, J.; Sato, K. *Curr. Opin. Struct. Biol.* **1998**, *8*, 417.

(38) van Soest, T. C.; de Jong, S.; Roijers, E. C. *J. Am. Oil Chem. Soc.* **1990**, *67*, 415.

(39) de Jong, S.; van Soest, T. C. *Acta Crystallogr., Sect. B: Struct. Sci.* **1978**, *34*, 1570.

(40) de Jong, S.; van Soest, T. C.; van Schaick, M. A. *J. Am. Oil Chem. Soc.* **1991**, *68*, 371.

(41) The coefficient corresponding to the two-chain or three-chain layer of a molecular pair of TAG molecules has to be multiplied by 1 or by 2/3, producing 5.62 and 5.73 Å, respectively.

(42) Filer, L. J., Jr.; Sidhu, S. S.; Daubert, B. F.; Longenecker, H. E. *J. Am. Chem. Soc.* **1946**, *68*, 167.

(43) Fahey, D. A.; Small, D. M.; Kodali, D. R.; Atkinson, D.; Redgrave, T. G. *Biochemistry* **1985**, *24*, 3757.

(44) Revaluation of the α_1-phase model shows that if there was a $T_{\|}$ subcell in this phase (although it is not confirmed by observed short *d*-spacings, Figure 6), then the tilt of acyl chains, in accordance with the formula for the long spacing of two-chain β phases of saturated TAGs, $L = (n + 6.62)/3c_s \sin \tau$, has to be $\tau_{\alpha_1} = 72.7°$ (Figure 10b), which is very close to the tilt angle of the StOSt molecule in the γ phase. The obtained angle is also close to the theoretical value of 71° suggested for C-type methyl terrace.[33] This type of terracing is not the favorable one for monosaturated TAGs; however, its formation was found in these TAGs. Probably, this preorientation of StOSt molecules in the two-chain layer of the α_1 phase takes place during the transformation into the three-chain layer of the γ phase.